

## Characterization of oxide films by MeV ion beam techniques

This article has been downloaded from IOPscience. Please scroll down to see the full text article.

2008 *J. Phys.: Condens. Matter* 20 264010

(<http://iopscience.iop.org/0953-8984/20/26/264010>)

[View the table of contents for this issue](#), or go to the [journal homepage](#) for more

Download details:

IP Address: 129.252.86.83

The article was downloaded on 29/05/2010 at 13:17

Please note that [terms and conditions apply](#).

# Characterization of oxide films by MeV ion beam techniques

M Döbeli<sup>1</sup>

Ion Beam Physics, Paul Scherrer Institute and ETH Zurich, 8093 Zurich, Switzerland

E-mail: [doebeli@phys.ethz.ch](mailto:doebeli@phys.ethz.ch)

Received 19 November 2007, in final form 21 February 2008

Published 9 June 2008

Online at [stacks.iop.org/JPhysCM/20/264010](http://stacks.iop.org/JPhysCM/20/264010)

## Abstract

MeV ion beam techniques can provide highly quantitative compositional analysis of surfaces and thin layers. This quantitativeness is due to the very well known elastic nuclear scattering cross-sections of MeV particles. The most commonly used techniques are Rutherford backscattering spectrometry and elastic recoil detection analysis. Owing to the energy loss of ions in the material, whole compositional depth profiles can be obtained in a single short measurement almost nondestructively. The sensitivity to oxygen can be enhanced by the use of nuclear resonances or forward scattering techniques. State-of-the-art ion beam analysis can determine thin film stoichiometries with an accuracy of 1% and a depth resolution in the low nm range.

An overview of the available techniques is given and illustrated with examples.

(Some figures in this article are in colour only in the electronic version)

## 1. Introduction

Complete characterization of thin films may include analysis of many different qualities of the material such as electrical, magnetic, optical, chemical or structural properties. One of the most basic tasks is the determination of the elemental composition and thickness of the film. This type of analysis can be achieved destructively by sputtering or ablation of the material combined with mass spectrometric methods. Nondestructive techniques use scattering of particles or radiation to determine the atomic species in the film. For those approaches where electromagnetic radiation or electrons are the probing species, interaction takes place via the electron shell of the sample atoms. As a consequence calculation of cross-sections is not always straightforward and secondary effects like absorption and fluorescence may affect accuracy. The same is true for low energy ion scattering where the probing projectiles do not fully penetrate the atomic shell. However, the determination of cross-sections becomes considerably easier if ions are scattered from target nuclei under large angles and at energies for which the distance of closest approach is clearly smaller than the radius of the lowest electron shell but still much larger than the range

of nuclear forces. In this case the interaction is of pure Coulomb type and the simple Rutherford formula is a good approximation [1]. If the energy range of ions is restricted to a certain window, electronic screening corrections are small and can be calculated by simple approximations [1]. No corrections for the molecular electronic structure have to be taken into account and virtually no ‘matrix effect’ exists. On the contrary, the small and almost continuous energy loss caused by collisions of the ions with electrons of the sample material can be utilized to calculate the depth at which the scattering took place. For light ions of a few MeV this electronic energy loss per path length is often not big enough to induce considerable damage to the target material. In addition, the cross-section for hard collisions that can displace atoms in the sample is small and therefore the techniques can frequently be regarded as virtually nondestructive. The high absolute accuracy, the simplicity of interpretation and the large amount of information that can be gained within a very short measurement time are the reasons why MeV ion beam techniques are popular despite the fact that a small particle accelerator has to be operated to perform the measurement.

In the following, the two most important ion beam analysis methods, Rutherford backscattering spectrometry (RBS) and elastic recoil detection analysis (ERDA) are discussed with regard to oxide film analysis. More general information on the topic of MeV ion beam analysis can be found in [1–3].

<sup>1</sup> Address for correspondence: IPP HPK H32, ETH-Hönggerberg, CH-8093 Zurich, Switzerland.

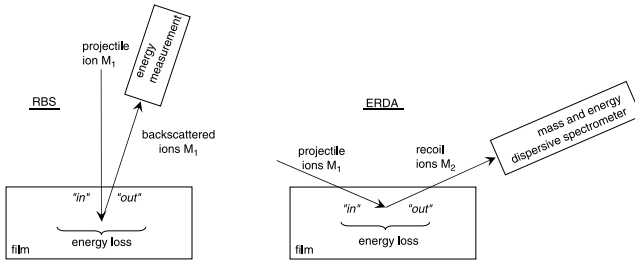


**Figure 1.** Schematics of the geometric set-up of a Rutherford backscattering (left) and an elastic recoil detection analysis (right) measurement.

## 2. Rutherford backscattering spectrometry (RBS)

The most widespread ion beam analysis technique is RBS. Figure 1 schematically shows the geometry of an RBS set-up. The sample surface is bombarded by a monoenergetic beam of light projectile ions and the energy of elastically scattered beam particles is measured in a detector under a backward angle [2]. The fraction of energy carried by the scattered particle is a monotonic and unambiguous function of the mass of the target nucleus, so elements in the sample can be identified by their mass. For scatterings that take place below the sample surface the final energy of the detected particle is shifted by the amount of energy which is continuously lost to electrons on the way in and out of the sample. Therefore the measured energy is at the same time a mass and a depth scale for the sample composition. In other words, the energy spectrum of backscattered projectiles is a superposition of the concentration depth profiles of all elements present in the target that are heavier than the beam particles. The scattering cross-section is proportional to the square of the atomic number of the target species, therefore the sensitivity to heavier sample elements is greatly enhanced. The cross-section is also proportional to  $1/E^2$  where  $E$  is the projectile energy. As the signal height in an RBS energy spectrum is proportional to the scattering cross-section divided by the specific energy loss of the projectile [2] RBS spectra of thick layers or bulk samples of uniform composition generally increase towards lower energy due to the continuous energy loss along the track of the incident particle and the consequent increase of the scattering cross-section with depth.

Under standard conditions  ${}^4\text{He}$  at an energy of 2 MeV is used as projectile and backscattered particles are detected by a simple Si detector. Figure 2 shows an RBS spectrum of a 250 nm  $\text{TiO}_2$  film deposited on a carbon substrate taken under standard conditions at a scattering angle of  $165^\circ$  to the incident beam direction. This example shows the main features of a thin film RBS spectrum. Since the layer is thin enough the titanium, the oxygen and the substrate signal are completely separated. For each element the right-hand edge of the spectrum corresponds to the signal coming from the surface and the depth scale points to the left. The solid line is a simulation of the spectrum by the RUMP software [4]. As mentioned above the scattering cross-sections and energy loss processes are so well known that simulations agree with experimental data to a very high degree and calibration

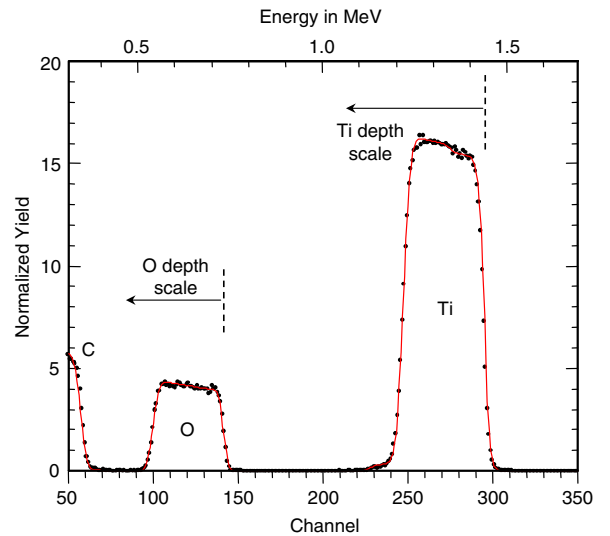


**Figure 2.** 2 MeV  ${}^4\text{He}$  RBS spectrum of a 250 nm thick  $\text{TiO}_2$  film on a carbon substrate. The solid line is a simulation [4]. Direction of depth scales for Ti and O concentration profiles is indicated by arrows.

standards are not required at all. Therefore interpretation of measurements is usually done by a fit or comparison with simulations [4–6].

For thin layers on light substrates with well separated signals, as in figure 2, the total number of events in the individual parts of the spectrum is proportional to the number of atoms per  $\text{cm}^2$  of the corresponding elemental species. In this case the stoichiometric ratio can be calculated with very high accuracy which is approximately 1% or below, depending mainly on how well the scattering cross-section can be calculated for the projectile energy used in the experiment. The necessary counting statistics can normally be reached without difficulties. In the example of figure 2 several hundred thousand backscattering events have been acquired within a measurement time of 5 min. The resulting stoichiometry of the sputter-deposited titanium oxide film was  $\text{TiO}_{1.95 \pm 0.02}$ .

For the determination of the film thickness there is redundant information. On the one hand it can be calculated from the width of the box spectra of all species in the film via the specific energy loss values in the material. In RBS analysis software these specific energy losses are usually calculated by semi-empirical models [7] with an accuracy of 3–5%, depending on the projectile–target atom combination. On the other hand the areal density of the layer can be calculated from the total number of events in the elemental spectra if the detector solid angle and the number of incident beam particles are exactly known. Especially with highly insulating oxides the precise integration of beam current can be a problem and the degree of accuracy of both techniques is comparable. In any case the thickness is always obtained as an areal density of atoms. A value for the density of the film material has to be assumed to derive the thickness in nm. For the film in figure 2 the areal density was determined to  $(2.40 \pm 0.08) \times 10^{18}$  at  $\text{cm}^{-2}$  corresponding to a thickness of  $(252 \pm 8)$  nm with a  $\text{TiO}_2$  bulk density of  $4.23 \text{ g cm}^{-3}$ . This result does

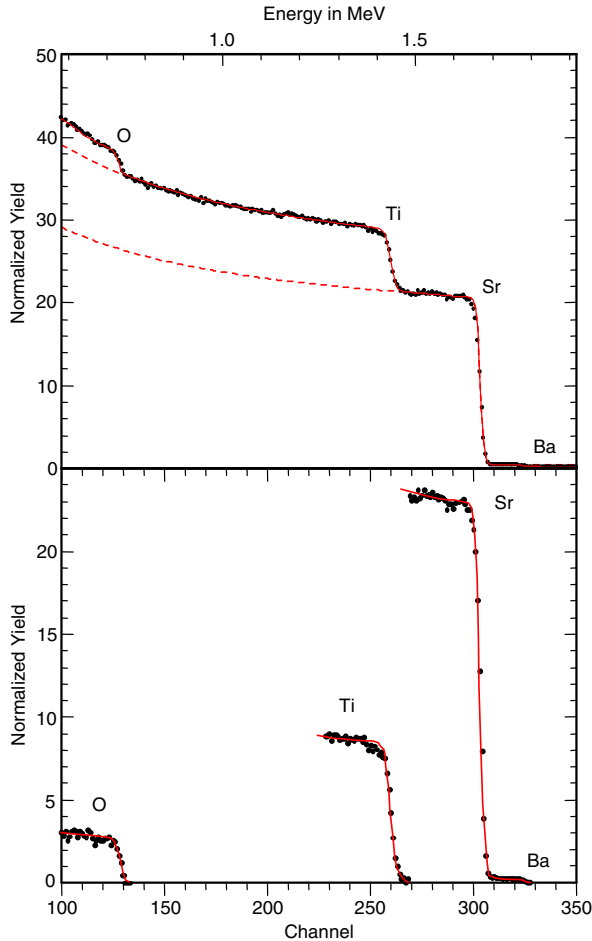


**Figure 3.** 2 MeV  ${}^4\text{He}$  RBS spectrum of a thick ( $>1.5\text{ }\mu\text{m}$ ) strontium titanate ( $\text{SrTiO}_3$ ) film. The solid line is a simulation [4]. Top: original spectrum. Dashed lines indicate the continuation of the signal of heavier elements. Bottom: background of heavier elements has been subtracted from elemental edges.

not include the uncertainty of the film density. For thick layers and bulk samples the profiles of individual elements overlap and the ratio between atomic concentrations can only be determined via the height of elemental steps in the spectrum. In figure 3 (top) an RBS spectrum of a thick ( $>1.5\text{ }\mu\text{m}$ ) strontium titanate film grown by pulsed laser deposition [8] is shown. The dashed lines indicate the continuation of the Sr and Ti spectrum below the signal of the lighter elements. In order to facilitate data analysis the background produced by heavier elements can be subtracted from the spectral part of lighter elements so that only the edges of each elemental step remains [9] (figure 3, bottom). In contrast to the well isolated peaks of figure 2 the stoichiometry cannot be determined from peak integrals but is given by the height of the plateaus. Since the energy loss per path length in the material enters the calculation of the spectrum height [2] the accuracy is lower in this case. As stated above, the error of calculated energy losses is between 3 and 5% [7], therefore the accuracy of the stoichiometric ratios is of the same order. However, if samples of similar composition are compared the measured relative differences in elemental concentrations can be much preciser.

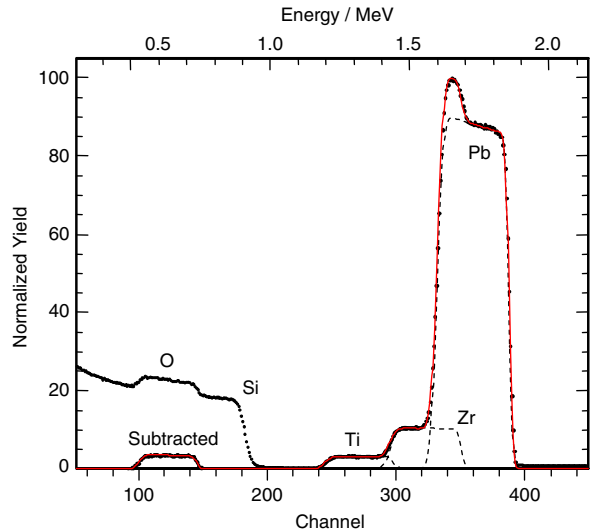


**Figure 4.** 2 MeV  ${}^4\text{He}$  RBS spectrum of a 280 nm thick lead zirconate titanate (PZT) film on Si. The solid line is a RUMP [4] simulation. Dashed lines indicate the signals from individual elements as obtained by RUMP. The silicon substrate signal has been subtracted to obtain the oxygen spectrum. The composition as determined by the simulation is  $\text{PbZr}_{0.480\pm 0.015}\text{Ti}_{0.480\pm 0.015}\text{O}_{3.09\pm 0.09}$  with a thickness of  $(277 \pm 9)$  nm.

In the example shown in figure 3 the resulting stoichiometry is  $\text{Sr}_{0.96}\text{Ti}_{1.04\pm 0.03}\text{O}_{2.65\pm 0.09}$ . Here the sum of the stoichiometric indices of Sr and Ti has been fixed to 2. A strontium titanate substrate sample that was measured for comparison showed a composition of  $\text{Sr}_{1.0}\text{Ti}_{0.99\pm 0.03}\text{O}_{2.95\pm 0.09}$ . As a side-effect an admixture of 0.3% Ba was detected in the layer. Due to the strongly enhanced scattering cross-section the sensitivity to traces of heavy elements in lighter matrices can be on the order of 10–100 ppm.

The most complex spectra are obtained for films of intermediate thickness for which RBS can still ‘look through’ the whole layer but the signals of the constituent elements overlap. An example of this type is shown in figure 4 for a 280 nm thick lead zirconate titanate (PZT) film on silicon. In this case a simulation is necessary for an unambiguous interpretation of the spectrum. The composition can still be extracted with rather high precision (see figure caption) but an experimental technique, such as ERDA, able to separate the individual elemental profiles would be of clear advantage.

### 3. Resonant scattering

For oxides with heavy metal constituents the background below the oxygen signal is often so massive that a precise determination of the step height becomes problematic (see figure 3). This became most obvious shortly after the discovery of high temperature superconductors when the oxygen non-stoichiometry had to be determined as precisely as possible. Direct measurement of the oxygen concentration in thin films with alternative techniques is equally hampered by low cross-sections or low energies of characteristic electron and photon emission. In elastic backscattering of MeV ions the scattering

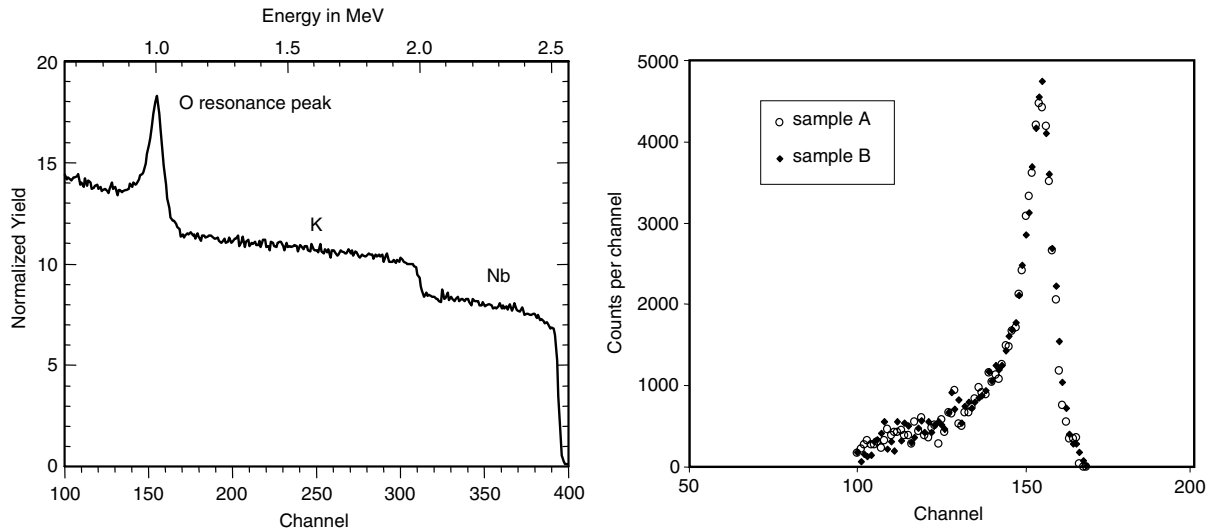


**Figure 5.** Determination of the oxygen concentration in a thick  $\text{KNbO}_3$  film by  $^{16}\text{O}(\alpha, \alpha)^{16}\text{O}$  resonance scattering at 3.05 MeV He beam energy. Left: total spectrum showing oxygen resonance peak. Right: comparison of the background-subtracted resonance peaks for two samples with a 3% different oxygen content. Reproduced with permission from [13]. Copyright 2006, Elsevier.

cross-section can be greatly enhanced for certain elements by raising the beam energy above the Rutherford region. In the case of oxygen there is the well known  $^{16}\text{O}(\alpha, \alpha)^{16}\text{O}$  resonance at 3.05 MeV beam energy for which the scattering cross-section at an angle of  $168^\circ$  is about 25 times larger than the Rutherford value [10–12]. With this technique even small amounts of oxygen can be detected with good accuracy. By fine-tuning of the beam energy the depth below the sample surface at which the resonance takes place can be selected and thus the oxygen concentration can be probed as a function of depth.

In figure 5 (top) a backscattering energy spectrum under resonant conditions of a thick potassium niobate film grown by liquid phase epitaxy [13] is shown. The area under the well visible resonance peak is proportional to the oxygen concentration at the chosen depth. Since the resonant yield of backscattered particles in the detector is very sensitive to the experimental set-up, very accurate absolute results can only be obtained by comparison with spectra of standard samples taken under identical conditions. Figure 5 (right) illustrates that even small changes in oxygen concentration can be determined by this technique. The graph shows the oxygen resonance peak of the potassium niobate sample described in the top figure in comparison with the peak obtained from an identical film which was treated under reducing atmosphere. The measured oxygen ratio between the unreduced and reduced sample is  $1.03 \pm 0.01$ .

#### 4. Elastic recoil detection analysis (ERDA)

In most cases the quantification of heavy metal constituents in oxides poses no problem. However the accurate analysis of oxygen and light metal stoichiometry and admixtures of e.g. hydrogen, carbon or nitrogen is less straightforward. In this respect RBS clearly suffers from the small scattering cross-sections of light elements and the sometimes huge background

from heavy sample constituents. Both these drawbacks can be overcome if not the backscattered projectile ions but the elastically forward scattered recoil atoms of the sample material are analyzed. This technique is called elastic recoil detection analysis (ERDA).

A clear distinction has to be made between ERDA and secondary ion mass spectrometry (SIMS). Both techniques use a primary ion beam to produce ionized secondary atoms of the target material. However, the energy range is completely different. In SIMS, sputtering and especially ionization of secondary atoms are complicated processes which delicately depend on the sample composition and structure. This severely hampers quantification. In ERDA, though, the interaction is the same as in RBS and takes place in the empty space around the nucleus. If the projectile energy is chosen properly scattering cross-sections are again well known. For low beam energies screening corrections exist [14, 15] and standardless quantification is possible with an accuracy of a few per cent. As described for RBS the energy loss of primary and recoiling ions can be used to establish a depth scale for concentration profiles. The number of primary ions needed for a measurement is much smaller than that necessary for a whole SIMS depth profile. As long as very high values of electronic energy loss are avoided [16] sputtering coefficients are low, and the analysis is much less destructive than SIMS. A whole depth profile can be obtained within a few minutes. In contrast to RBS the mass or atomic number of the detected particles has to be determined. This necessitates more sophisticated spectrometers but has the huge advantage that separate energy spectra and thus concentration depth profiles are obtained simultaneously for each atomic species in the sample. Figure 1 schematically shows the geometry of an ERDA set-up. Usually, a relatively heavy ion (e.g.  $^{127}\text{I}$ ,  $^{197}\text{Au}$ ) serves as incident projectile suited to transfer enough momentum to all types of target atoms. Glancing angles are used for the incident beam as well as for detection of recoils. The spectrometer has not only to

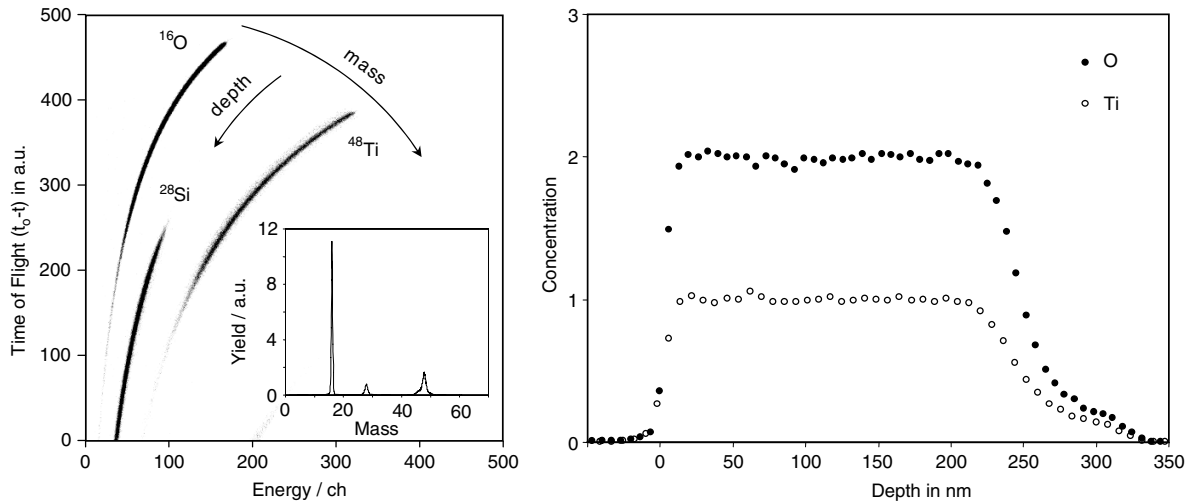


**Figure 6.** ERDA spectrum of a  $\text{TiO}_2$  layer on a silicon substrate. Projectile beam was 12 MeV  $^{127}\text{I}$ . Particles were identified by a combination of a ToF spectrometer with a gas ionization chamber [17]. Left: bi-parametric plot of the flight-time versus total energy of the recoiling target atoms. The inset shows the derived mass spectrum. Right: depth profiles of titanium and oxygen calculated from corresponding energy spectra.

discriminate between different recoiling target species but has also to identify or suppress scattered projectile ions which can be a problem.

There is a number of possible combinations of magnetic, electrostatic, time-of-flight (ToF), solid state, and gas ionization detectors that can be used to form an energy and mass dispersive spectrometer. In addition, there is much more flexibility in the choice of projectile mass and energy than in RBS. Therefore, it is beyond the scope of this article to discuss the optimization of experimental parameters for a given analytical problem.

As a first example an ERDA spectrum of a  $\text{TiO}_2$  layer on silicon substrate is presented in figure 6. 12 MeV  $^{127}\text{I}$  ions were used as projectile beam and recoils were identified by a combination of a ToF and a gas ionization detector [17]. In a bi-parametric plot of flight-time versus recoil energy each mass forms a line (usually called ‘banana’) following the simple relationship  $E = \frac{1}{2}mv^2 = \frac{1}{2}m(l/t)^2$ , where  $l$  is the flight path length and  $t$  the time-of-flight. Particles scattered from the surface have the highest energy and appear at the upper right end of a ‘banana’. Recoils originating from greater depth have less energy and appear further down along the ‘banana’. Thus the bi-parametric spectrum represents the individual depth profiles of all atomic species in the sample. By selecting a single ‘banana’ the energy spectrum of the corresponding recoil particles can be calculated and transformed into the depth profile by appropriate software (e.g. NDF [5]) that corrects for scattering cross-sections and energy loss in the material. The resulting compositional depth profile for the  $\text{TiO}_2$  layer is shown in the right part of figure 6. Due to the good resolution of a ToF system and especially because of the large specific energy loss of the iodine projectiles in the sample material the depth resolution, usually a few nm, is considerably better than with standard RBS. In return, the heavy projectiles and the slow recoils tend

to scatter more than once along their path which leads to a distortion of the profiles, manifested by the tails at the low energy end of the spectrum [18] which are a pure artifact of the measurement but can easily be mistaken for diffusion effects or film roughness.

In a different approach, the two-dimensional spectrum can be converted into a mass spectrum by the simple relation given above (figure 6, left inset) [17]. This gives semi-quantitative information on the target composition and is especially useful to determine small traces of elements. Atomic fractions down to  $10^{-3}$  or even lower can be detected, depending on experimental parameters. The mass spectrum can be evaluated quantitatively if proper corrections for scattering cross-sections and energy loss are performed.

In figure 7 an ERDA measurement of a  $\text{LiMn}_2\text{O}_4$  layer (thickness  $> 200$  nm) on silicon is displayed. Experimental parameters were the same as for the analysis of the  $\text{TiO}_2$  layer. Again, the raw bi-parametric data, the mass spectrum and the depth profiles for Li, Mn and O are shown. Under the chosen beam conditions the depth of analysis is smaller than the layer thickness. While this measurement would have been impossible by RBS because of the low mass and scattering cross-section of lithium, ERDA does not have any limitations in this respect. All light elements down to hydrogen can be detected and cross-sections do not vary strongly across the periodic table.

Since this type of spectrometer is mass dispersive, isotope-specific depth profiles can be obtained with ease for all isotopes without nuclear isobars, which is the case for all light elements in the periodic table from hydrogen to chlorine. This can be utilized to perform tracer experiments with isotope-enriched substances. In particular, the two oxygen isotopes  $^{16}\text{O}$  and  $^{18}\text{O}$  can be tracked to investigate oxidation processes at surfaces and in thin films [19]. Similarly, the quantification of the nitrogen content in oxynitrides is straightforward [20, 8].

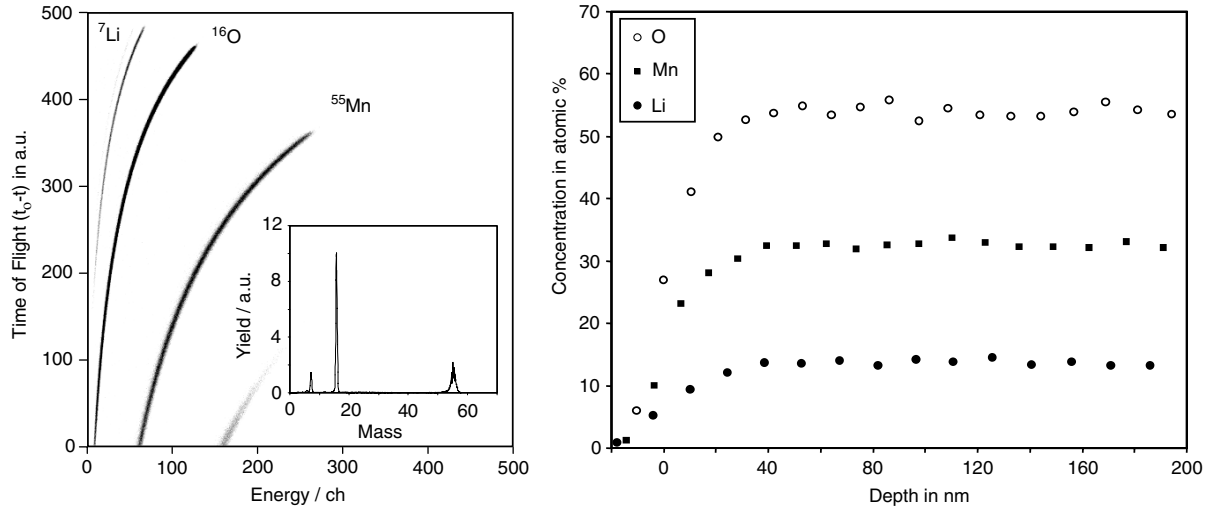


**Figure 7.** ERDA spectrum of a more than  $0.2 \mu\text{m}$  thick  $\text{LiMn}_2\text{O}_4$  layer. Experimental conditions were the same as in figure 6. Left: bi-parametric plot of the flight-time versus total energy of the recoiling target atoms with corresponding mass spectrum. Right: derived depth profiles of manganese, lithium and oxygen.

## 5. High resolution techniques

With standard detectors of 10–15 keV energy resolution (FWHM) RBS has a typical depth resolution of 10–20 nm. By using glancing incidence angles this resolution can be improved by a factor of about 3. For ERDA glancing incidence angles are a necessity because of the forward scattering geometry, in addition heavier projectiles with larger specific energy loss are used. Therefore the depth resolution is generally better for ERDA than for RBS. If high resolution spectrometers are applied (magnetic, electrostatic, ToF) the depth resolution is considerably improved [20]. For both techniques sub-nm resolution can be obtained and for specially prepared sample surfaces monolayer resolution has been proved [21–23].

Due to elastic scattering kinematics, the mass dependence of the energy of backscattered projectiles decreases with target mass and consequently the mass resolution is considerably diminished for heavy elements. With a state-of-the-art silicon detector a mass difference of 1 u can be discriminated by RBS only for elements up to approximately Ca. If neighboring heavy elements have to be identified again high resolution spectrometers may be used. Alternatively, ions heavier than He can serve as projectiles. This greatly enhances the mass resolution of the technique, but necessitates special detectors, as silicon is degrading fast under heavy ion irradiation [24]. In the case of ERDA also a significant instrumental effort is needed to maintain unit mass resolution throughout the periodic table. For both, RBS and ERDA, an additional option is to look at the emitted characteristic x-rays under MeV ion irradiation (particle induced x-ray emission, PIXE). This can be done simultaneously with the RBS measurement [25] or in a separate measurement with a proton beam [26].

Figure 8 shows an RBS spectrum of an yttria-stabilized zirconia layer on  $\text{Al}_2\text{O}_3$ . While the thickness of the layer and the oxygen stoichiometry can be well determined by standard RBS, the yttrium (1 isotope at 89 u) and zirconium

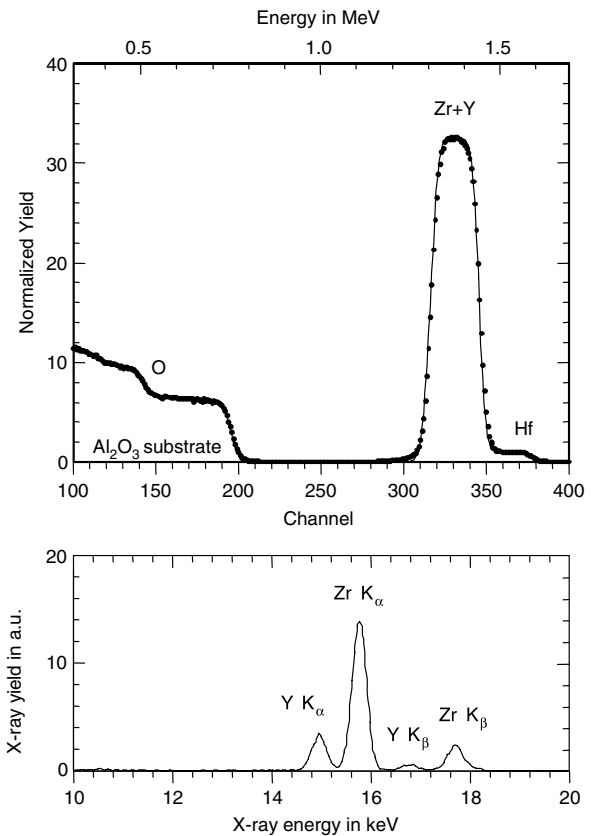


**Figure 8.** 2 MeV  ${}^4\text{He}$  RBS spectrum of a 140 nm thick film of yttria-stabilized zirconia on  $\text{Al}_2\text{O}_3$ . The solid line is a RUMP simulation [4]. Hf is a contaminant of Zr. The Y/Zr ratio has been determined to 0.18 by PIXE with 3 MeV protons (bottom). Adapted from [27].

(5 isotopes between 90 and 96 u) cannot be separated. An additional PIXE measurement with 3 MeV protons yields the Y/Zr ratio of 0.18 by the well separated characteristic

K-lines in the x-ray spectrum taken by a Si(Li) detector (figure 8, inset). An important advantage of PIXE over x-ray analysis with electron microprobes is the almost complete absence of bremsstrahlung background, considerably raising the sensitivity [26]. Concerning the quantitativeness of this technique similar caution has to be applied regarding absorption and fluorescence of the emitted x-rays as with an electron microprobe.

## 6. Summary

The foremost advantage of MeV ion beam analysis of surfaces is its high accuracy which can be reached without calibration standards. Composition profiles can be obtained in minutes with an accuracy of the depth scale of better than 5%. With high resolution spectrometers a depth resolution below 1 nm is reached at the sample surface. For thin layers the experimental error of stoichiometry measurements is less than 1%. For thick layers and bulk samples this error is between 3 and 5%. However, accuracy and sensitivity may also depend on film qualities such as surface roughness and on the composition of the substrate material. For epitaxial layers ion channeling along crystal directions has to be carefully avoided. For the analysis of metal oxide films RBS is an excellent technique to exactly determine the heavy components while ERDA is much better suited to analyze the oxygen and light element content. Among all available techniques it is therefore a favorite for the direct determination of oxygen stoichiometry [20]. ERDA is clearly more powerful than RBS but is also more demanding with respect to experimental equipment and data analysis. While RBS with MeV helium ions is practically nondestructive a certain care has to be observed with ERDA.

The high quantitativeness of ion beam analysis comes mainly from the fact that the electronic structure of the sample material has virtually no influence on the scattering cross-section. By the same reason, however, it is not possible to obtain any information on the chemical binding state of atoms.

## References

- [1] Tesmer J R and Nastasi M (ed) 1995 *Handbook of Modern Ion Beam Materials Analysis* (Pittsburgh, PA: MRS)
- [2] Chu W K, Mayer J W and Nicolet M A 1978 *Backscattering Spectrometry* (New York: Academic)
- [3] Feldman L C and Mayer J W 1986 *Fundamentals of Surface and Thin Film Analysis* (Amsterdam: North-Holland)
- [4] Doolittle L R 1986 *Nucl. Instrum. Methods B* **15** 227
- [5] Barradas N P, Jeynes C and Webb R P 1997 *Appl. Phys. Lett.* **17** 291
- [6] Mayer M 1999 *AIP Conf. Proc.* **475** 541
- [7] Ziegler J F, Biersack J P and Littmark U 1985 *The Stopping and Range of Ions in Solids* (New York: Pergamon)  
Computer code available at [www.srim.org](http://www.srim.org).
- [8] Marozau I, Döbeli M, Lippert T, Logvinovich D, Mallepell M, Shkabko A, Weidenkaff A and Wokaun A 2007 *Appl. Phys. A* **89** 933
- [9] Döbeli M 2006 *Nucl. Instrum. Methods B* **249** 800
- [10] Mezey G, Gyulai J, Nagy T, Kotai E and Manuba A 1976 *Ion Beam Surface Layer Analysis* ed O Meyer, G Linker and F Käppeler (New York: Plenum) p 303
- [11] Battistig G, Kennedy E F, Revesz P, Gyulai J, Kadar G, Gyimesi J, Drozdy G and Vizkelethy G 1986 *Nucl. Instrum. Methods B* **15** 372
- [12] Blanpain B, Revesz P, Doolittle L R, Purser K H and Mayer J W 1988 *Nucl. Instrum. Methods B* **34** 459
- [13] Choubey A, Döbeli M, Bach T, Montemezzani G, Günther D and Günter P 2006 *J. Cryst. Growth* **297** 87
- [14] Andersen H H, Besenbacher F, Loftager P and Moller W 1980 *Phys. Rev. A* **21** 1891
- [15] L'Ecuyer J, Davies J A and Matsunami N 1979 *Nucl. Instrum. Methods* **160** 337
- [16] Dollinger G, Boulouednine M, Bergmaier A and Faestermann T 1998 *Nucl. Instrum. Methods B* **136–138** 574
- [17] Kottler C, Döbeli M, Glaus F and Suter M 2006 *Nucl. Instrum. Methods B* **248** 155
- [18] Giangrandi S, Arstila K, Brijs B, Sajavaara T, Vantomme A and Vandervorst W 2007 *Nucl. Instrum. Methods B* **261** 512
- [19] Montenegro M J, Conder K, Döbeli M, Lippert T, Willmott P R and Wokaun A 2006 *Appl. Surf. Sci.* **252** 4642
- [20] Brijs B, Deleu J, Conard T, De Witte H, Vandervorst W, Nakajima K, Kimura K, Genchev I, Bergmaier A, Goergens L, Neumaier P, Dollinger G and Döbeli M 2000 *Nucl. Instrum. Methods B* **161–163** 429
- [21] Kimura K, Ohshima K, Nakajima K, Fujii Y, Mannami M and Goosmann H-J 1995 *Nucl. Instrum. Methods B* **99** 472
- [22] Carstanjen H D 1998 *Nucl. Instrum. Methods B* **137** 1183
- [23] Dollinger G, Frey C M, Bergmaier A and Faestermann T 1998 *Nucl. Instrum. Methods B* **137** 603
- [24] Döbeli M, Haubert P C, Livi R P, Spicklemire S J, Weathers D L and Tombrello T A 1990 *Nucl. Instrum. Methods B* **47** 148
- [25] Beck L, Bassinot F, Gehlen M, Trouslard Ph, Pellegrino S and Levi C 2002 *Nucl. Instrum. Methods B* **190** 482
- [26] Johannsson S A E and Campbell J L 1988 *PIXE: A Novel Technique for Elemental Analysis* (New York: Wiley)
- [27] Heiroth S, Lippert Th, Wokaun A and Döbeli M 2008 *Appl. Phys. A* submitted